ELSEVIER

Physics of the Earth and Planetary Interiors 128 (2001) 223–241

PHYSICS OF THE EARTH AND PLANETARY INTERIORS

www.elsevier.com/locate/pepi

Paleomagnetism of late Archean rocks of Hamersley basin, Western Australia and the paleointensity at early Proterozoic

Ikuro Sumita*, Tadahiro Hatakeyama[1], Arata Yoshihara, Yozo Hamano

Department of Earth and Planetary Science, Graduate School of Science, University of Tokyo, Tokyo 113-0033, Japan

Received 7 September 2000; accepted 14 August 2001

Abstract

We report the results of paleomagnetic and rock magnetic measurements of late Archean rocks from Hamersley basin, Western Australia, and the paleointensity determination for early Proterozoic. Basalts and banded iron formations have two to four components of remanent magnetization, and have consistent directions for different localities, indicative of geomagnetic origin. Rock magnetic measurements of basalts reveal that the main magnetic mineral is a fine-grained magnetite present in ~10 ppm in mass, which do not alter when heated up to its blocking temperature. We interpret the stable component up to ~390 °C as the post-tilting thermal overprint from uplift at ≃2.0 Ga, and the higher temperature component as the pre-tilting thermoviscous remanence during burial metamorphism. From the Thellier type paleointensity experiments using the thermal overprint component, we obtain a mean virtual dipole moment (VDM) estimate of $(1.8–3.6) \times 10^{22}$ A m^2. This suggests that early Proterozoic was characterized by a 1 weak geomagnetic field of less than one-half of the present.

Keywords: Hamersley; Archean; Proterozoic; Basalts; Paleointensity

1. Introduction

The long-term evolution of the magnitude of the geomagnetic field (paleointensity), is an important source of information to constrain the dynamics and evolution of the Earth's core. Paleointensity data of Proterozoic and Archean period are particularly important, since they cover most of the Earth's history. However, we still have a very limited number of data, as can be seen from the paleointensity data compilation (e.g. Prévot and Perrin, 1992; Tanaka et al., 1995).

Hamersley basin is located in the north-west corner of Australia and is one of the best preserved Archean and Proterozoic regions on Earth. There have been several paleomagnetic and rock magnetic studies of the volcanic and sedimentary rocks of the Hamersley basin, together with those of the adjacent and older Pilbara craton (Porath and Chamalaun, 1968; Embleton, 1978; Embleton et al., 1979; McElhinny and Senanayake, 1980; Schmidt and Embelton, 1985; Schimdt and Clark, 1994). These studies have shown that quite a few of these rocks have remanent magnetization which dates back to Archean and Proterozoic times. However, there have been no reports on the paleointensity determination using these rocks. This paper extends the previous paleomagnetic studies on the Archean and Proterozoic rocks of Western Australia, and reports the first results of paleointensity

* Corresponding author. Present address: Faculty of Science, Department of Earth Sciences, Kanazawa University, Kanazawa 920-1192, Japan.

E-mail address: sumita@hakusan.s.kanazawa-u.ac.jp (I. Sumita).

[1] Present address: Institute for Study of the Earth's Interior, Okayama University, Misasa, Tottori 682-0193, Japan.

0031-9201/01/$ – see front matter
PII: S0031-9201(01)00288-6

determination using basalts of this region. This study is the continuation of the recent efforts to obtain a reliable paleointensity in the Archean and Proterozoic times, which have already been reported using rocks from Greenland (Morimoto et al., 1997) and Canada (Yoshihara and Hamano, 2000).

2. Geology and sampling

Hamersley basin formed during late Archean to early Proterozoic (2.8–2.4 Ga) and unconformably overlies the Pilbara craton (Hickman, 1983). It consists of volcanic (e.g. basalts, rhyolites) and sedimentary rocks (e.g. banded iron formations, hereafter BIFs) which were subject to only a weak metamorphism (lower than greenschist facies) and deformation.

Hand samples were sampled at two localities as shown in Fig. 1 and were oriented using a magnetic compass. Basalts were sampled at Considerable creek (seven pillow basalts at site COC: 117°52′E/23°06′S) and at Beasley river region (four hand samples from a lava flow at site BL: 117°07′E/22°52′S, five pillow basalts at site BP: 117°07′E/22°51′S). Blocks of BIFs were sampled at Beasley river region (site BM: 117°07′E/22°52′S). Considerable creek locality is along the road cutting with a good exposure of pillow basalts and sediments (Thorne and Tyler, 1994). Beasley river locality is along the Woongarra gorge cut by Beasley river. It has a good exposure of pillow basalts and lava flow at lower stratigraphy overlain by BIFs and sediments (Thorne et al., 1995). The bedding of this region is NW–SE strike with a southward dip, and was measured from the bedding plane of the sediments.

Basalts used in this study belong to Bunjinah Formation of Fortescue group. An U–Pb zircon age of 2690±16 Ma is obtained for Jeerinah Formation which

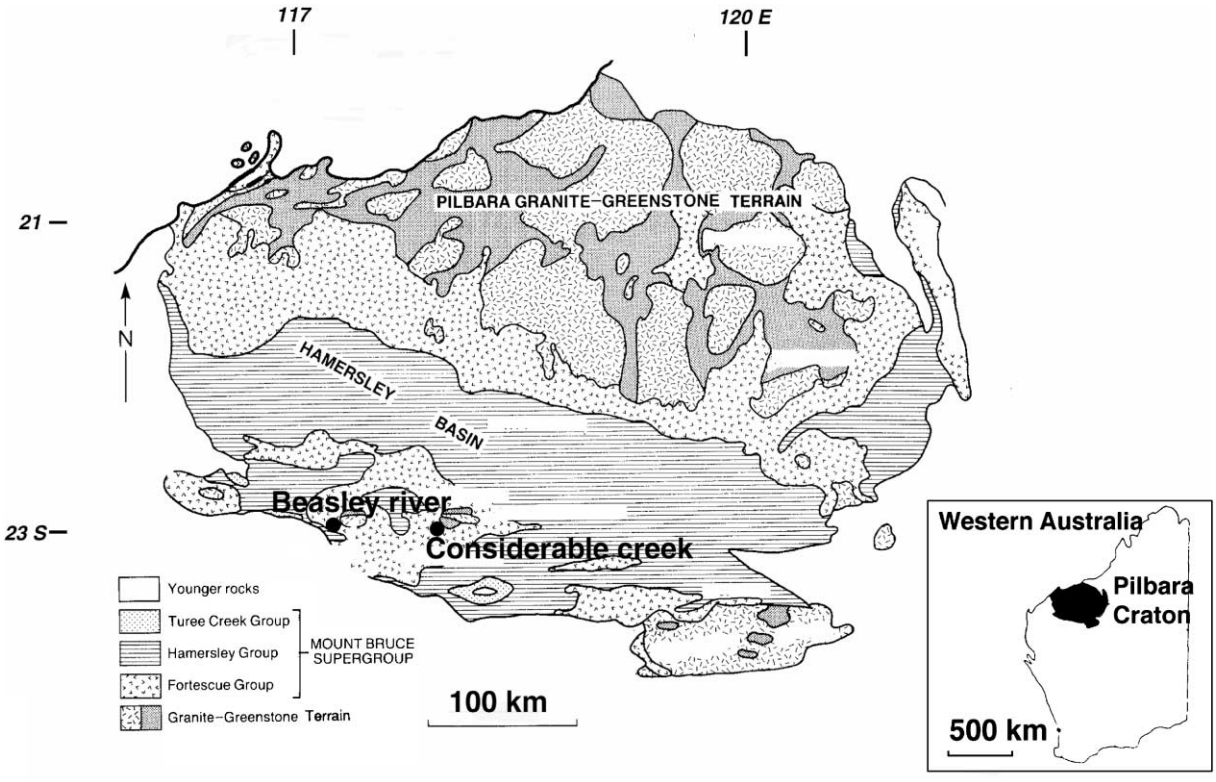

Fig. 1. Map of the Pilbara craton, showing the Pilbara granite-greenstone terrains in the north and the Hamersley basin in the south. The two sampling localities are indicated by solid circles.

conformably overlies the Bunjinah Formation (Arndt et al., 1991). The BIFs used in this study belong to Brockman iron formation of Hamersley group, and an U–Pb zircon age was obtained for the Dales Gorge member as 2470 ± 4 My (Trendall et al., 1990). These ages can be regarded as the formation or depositional ages of these rocks.

The metamorphic grade of these rocks is prehnite–pumpellyite to lowermost greenschist facies (Smith et al., 1982; Thorne and Tyler, 1994) and was confirmed from thin section observations (Ohta, Terabayashi, personal communication, 1997). The age of the last metamorphic event has been constrained from whole rock isotope systematics. From a basalt flow from a deep hole core of the Bunjinah formation, Nelson et al. (1992) obtained a Rb–Sr age of 2070 ± 114 Ma and a Pb–Pb age of 2063 ± 245 Ma. For Brockman iron formations, using riebeckite samples, Alibert et al. (1993) obtained a Sm–Nd age of 2140 ± 30 Ma. For a sample from the same formation, Erel et al. (1997) used a leaching method and obtained an U–Pb age of 2213 ± 250 Ma. These dates have been interpreted as the isotopic reset age by greenschist metamorphism, possibly accompanying hydrothermal activity.

3. Experimental methods

Core subsamples were prepared from the hand samples, and their remanent magnetizations were measured using 2G SQUID magnetometer which can measure specimens with magnetizations as low as of the order of 10^{-4} A/m. Thermal demagnetization and acquisition of thermal remanent magnetizations (TRMs) were done using Schonstedt's and Natsuhara's thermal demagnetizer. Alternating field demagnetization and an anhysteretic remanent magnetization (ARM) acquisition were carried out with an automated system attached to the SQUID magnetometer. Five to seven core specimens were heated for 10–25 min in the furnace at the target temperature and then cooled down under zero field for 20–30 min. Alternating field demagnetization of the shield was done after each TRM acqusition, to ensure that the residual magnetic field within the shield is maintained below 15 nT. Magnetic susceptibility was measured using a Bartington's susceptibility meter. Hysteresis curves, isothermal remanent magnetization (IRM) acquisition curves, temperature dependence of saturation magnetization were measured using vibrating sample magnetometer (Princeton Meas. Corp.) Microscopic observations of the samples were done using scanning electron microscope (SEM).

4. Paleomagnetic directions

The basalts are very weakly magnetized, having a natural remanent magnetization (NRM) intensity of the order of $\sim 10^{-3}$ A/m or less, which is 2 orders of magnitude smaller than saturation isothermal remanence magnetization (SIRM). Fig. 2a–g show the results of stepwise alternating field and thermal demagnetization for the basalts. Maximum unblocking temperature varies from about 490–590 °C, and about a half of the NRM is demagnetized by around 220–350 °C. The median destructive field is 25–30 mT. These samples are typically characterized by two to four components (directions in in situ coordinates): (1) a low temperature (<200 °C), low coercivity (<20 mT) VRM (viscous remanent magnetization) component, whose mean direction for the three localities ($D = -0.1^\circ$, $I = -40.1^\circ$, $\alpha_{95} = 14.2^\circ$), is close to that expected from the geocentric axial dipole (GAD) ($D = 0.0^\circ$, $I = -40.5^\circ$); (2) a mid-temperature (390 °C), mid-coercivity (<100 mT) component with a north-westerly declination and a shallow negative inclination; (3) a high-temperature (<500 °C) component, with a north-westerly declination and a shallow negative inclination (compared to (3), D is westward and I is deeper, in general); (4) a very high-temperature (520–590 °C) component with an easterly declination and a deep positive inclination.

Low- and mid-temperature (coercivity) components are present in all samples, but there are lesser number of samples with higher temperature components. For specimens shown in Fig. 2, COC4-12 (a), COC5-4 (b), BP1-11 (e) have components up to (2), BL1-21 (c), BL4-123 (d), have components up to (3), and BP1-312 (f), BP5-12 (g), have components up to (4). Specimens COC4-12 and BL4-123 have similar NRM intensity and multicomponent directions as compared to others of the same site, but their direction are different. These samples may have recently moved tectonically or have been misoriented, and we correct the paleomagnetic direction such that the low-temperature

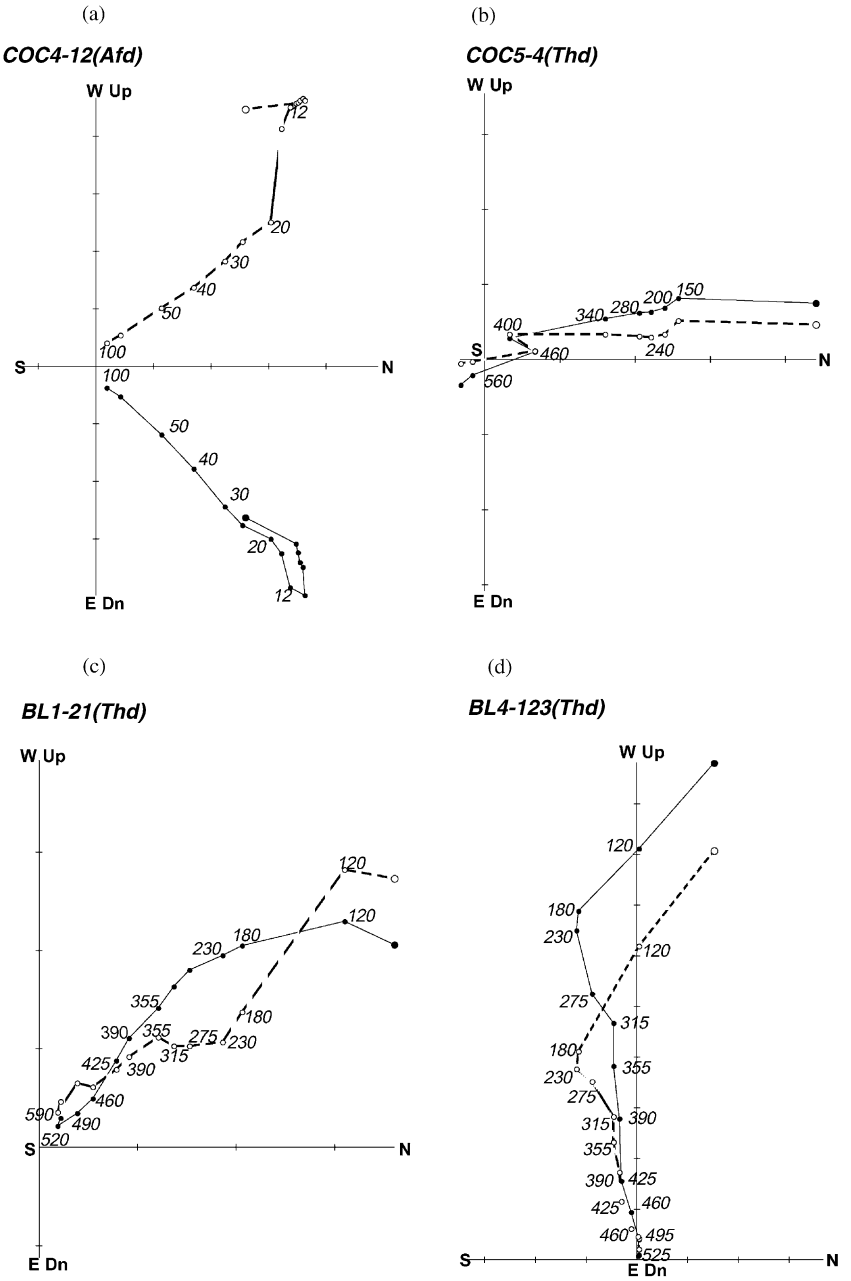

Fig. 2. Examples of alternating field (Afd) and thermal (Thd) demagnetization of (a–b): considerable creek pillow basalts (COC); (c–d): beasley river lava flow (BL); (e–g): beasley river pillow basalts (BP); (h–i): beasley river BIFs (BM). Solid (open) circles represent traces of the vectorial component projected on the NS–EW (NS–UD) plane. The numbers represent the peak demagnetizing field (in mT) or demagnetizing temperature given in °C.

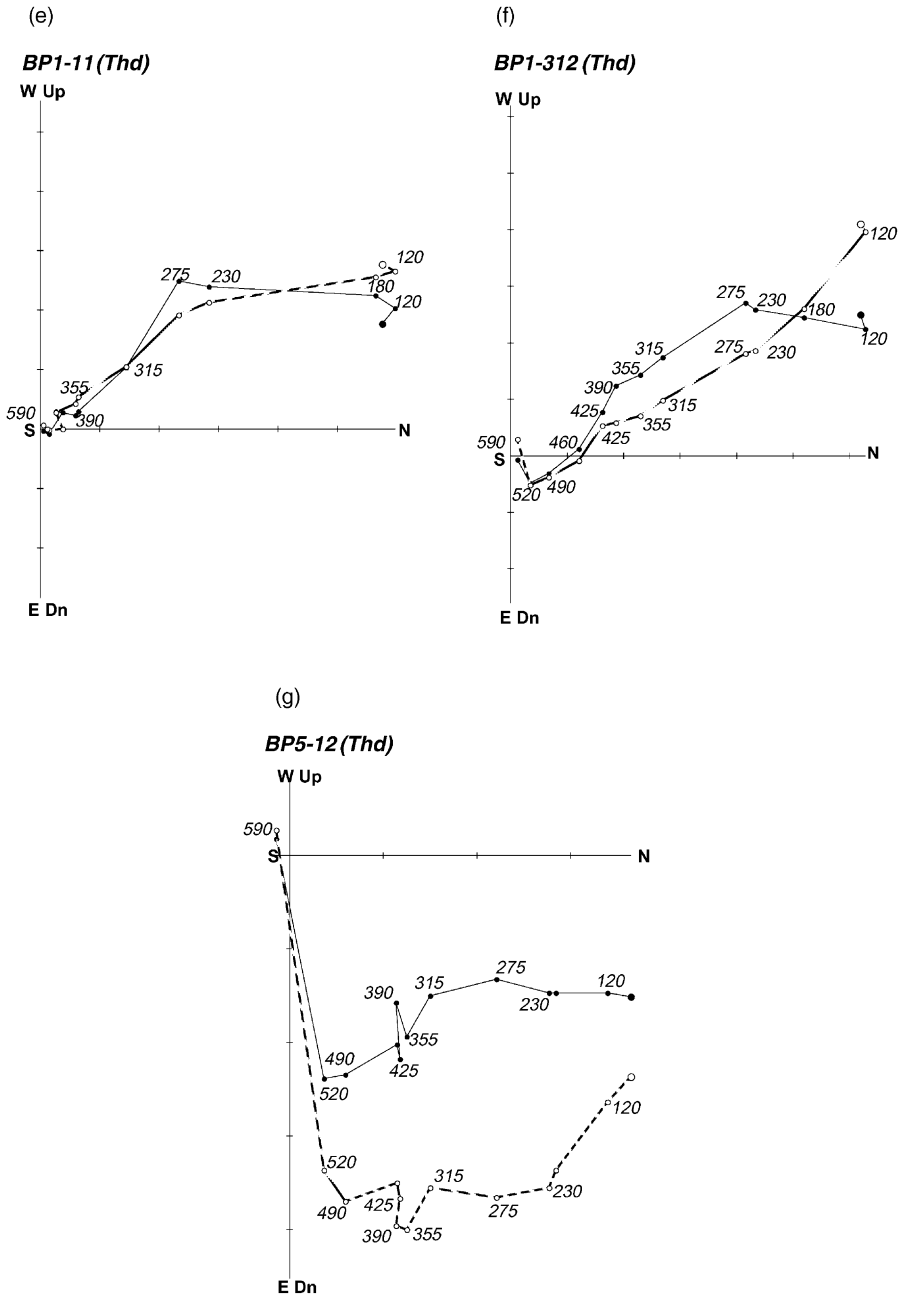

Fig. 2. (*Continued*).

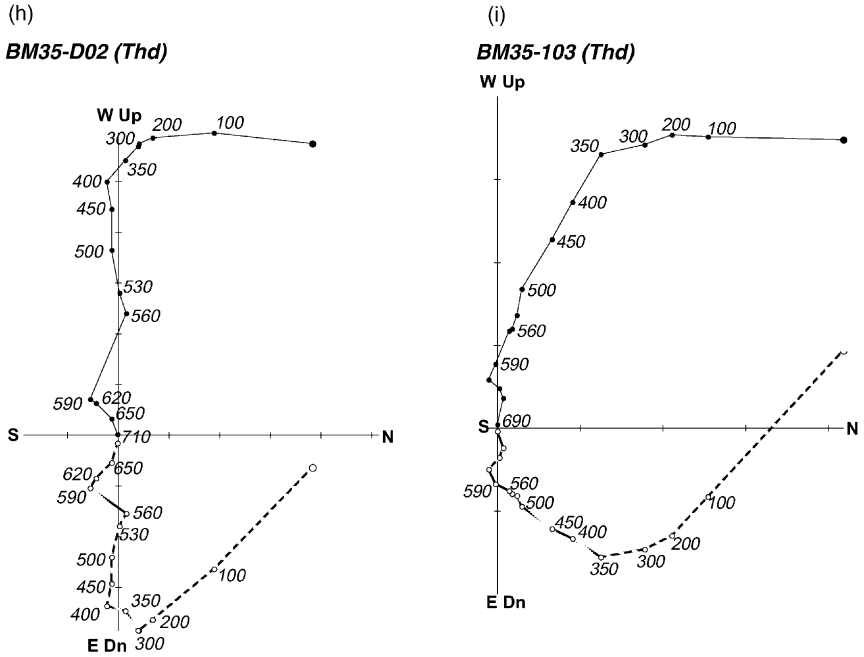

Fig. 2. (*Continued*).

component coincides with the present GAD field direction. We then find that the corrected direction of the mid- and high-temperature components coincide with those of other samples, verifying the validity of our correction.

Similarly, we determined the paleomagnetic direction using BIFs (Hatakeyama et al., 1997). BIFs used for the present study consist of alternating layers of iron oxide (magnetite and hematite) and chert, and have an average NRM intensity of 1.8×10^{-1} A/m. Cubic samples of 3–4 cm^3 were made from a block sample and an example of the result of stepwise thermal demagnetization is shown in Fig. 2h and i. These BIFs are characterized by the following components of magnetization. (1) A low-temperature ($<200\,^{\circ}C$) component having a direction close to the present GAD field. (2) A mid-temperature (<350–$400\,^{\circ}C$) component having a north-westerly declination and a generally shallow inclination. This component consists $<10\%$ of the total NRM intensity. (3) A high-temperature (<560–$590\,^{\circ}C$) component. (4) A very high-temperature ($<690\,^{\circ}C$) component of hematite origin. In this paper, we consider the origin of the mid-temperature component. A detailed analysis of other components together with their rock magnetic properties will be reported elsewhere.

A summary of the in situ and bedding corrected paleomagnetic direction of the basalts and BIFs are given in Table 1 and is plotted in Fig. 3a–c. For basalts, we used 1–10 specimens from each hand sample to determine the mean direction for each hand sample, and then calculated the site mean direction. For the BIFs, we used 29 specimens to determine the site mean direction of the mid-temperature component. We find that this direction is close to the mid-temperature component of the basalts, suggesting a common origin. The paleomagnetic directions are consistent within site and among different sites. This suggests that the NRM is geomagnetic in origin and not being affected by lightning, which is also supported by the small NRM:SIRM ratio.

For most samples, the high-temperature component is slightly westward and has a deeper negative inclination as compared to the mid-temperature component. The direction of the in situ mid-temperature component is close to the bedding corrected high-temperature

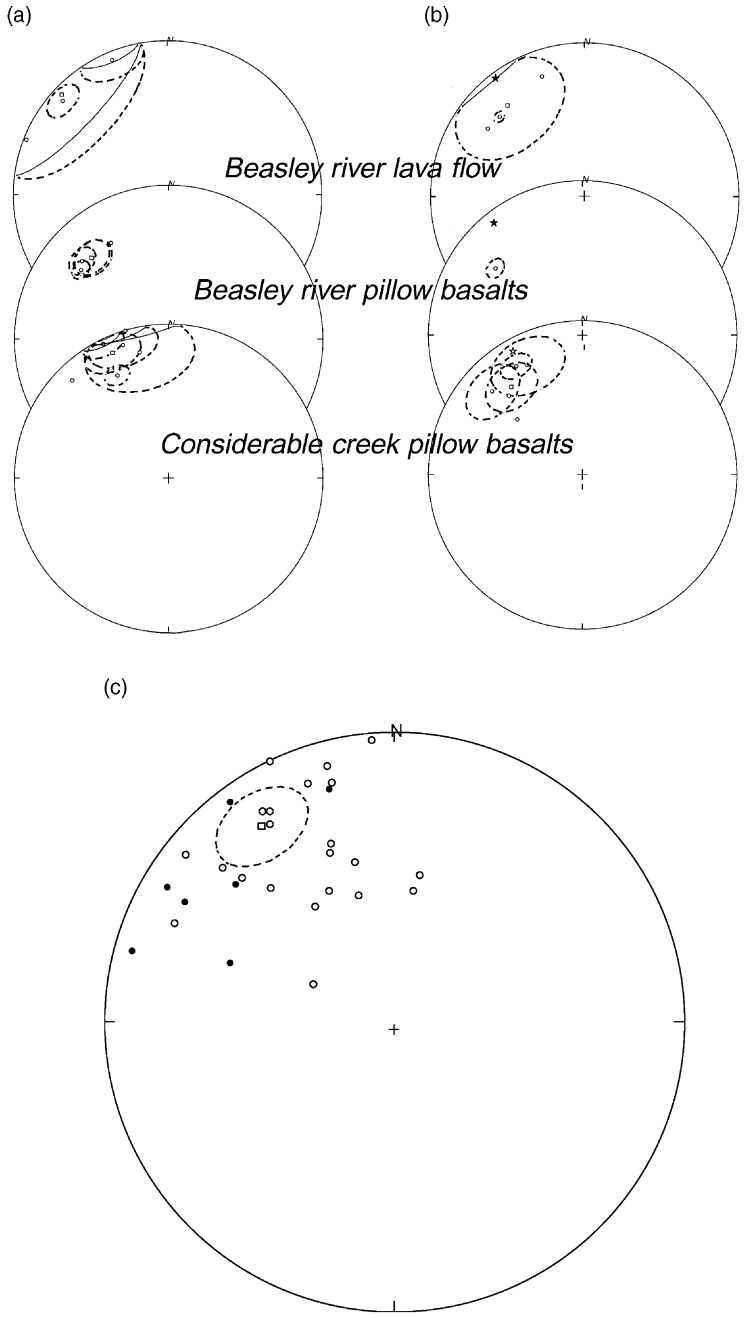

Fig. 3. Equal area plot of the paleomagnetic directions with confidence limits (α_{95}). Open (solid) marks indicate upward (downward) directions. Each circles represent the mean direction for each hand sample (cubic specimen for BIFs), squares represent the site mean direction: (a) mid-temperature components (in situ); (b) high-temperature components (in situ). Stars indicate the bedding corrected site mean direction. (c) Mid-temperature components (in situ) of the BIFs.

Table 1
A summary of paleomagnetic directions[a]

Locality	Site	Component	N_{used}/N_{total}	D (°)	I (°)	α_{95} (°)
Considerable creek	COC	L	5/7	0.1	−36.1	23.3
		M	6/7	335.8	−11.3	12.2
		H	6/7	320.9	−27.0	13.0
		H[b]	6/7	330.9	−8.5	13.0
Beasley river	BL	L	3/4	353.2	−49.4	8.6
		M	3/4	313.5	−5.8	36.9
		H	3/4	319.8	−22.9	27.3
		H[b]	3/4	322.8	4.0	27.3
Beasley river	BP	L	5/5	5.1	−34.5	19.7
		M	4/5	316.7	−27.5	9.3
		H	1/5	307.3	−29.5	4.9
		VH	3/5	70.3	46.9	12.9
		H[b]	1/5	321.6	7.2	4.9
		VH[b]	3/5	152.5	38.6	12.9
Beasley river	BM	M	29/33	325.8	−18.9	11.7

[a] D and I are site mean directions. For basalts (COC, BL, BP), N corresponds to separately oriented hand samples. For BIFs (BM), it corresponds to the number of cubic specimens. N_{used}: number of samples used for obtaining a site mean direction; N_{total}: total number of samples for each site.

[b] Bedding corrected directions are indicated, otherwise they are in in situ coordinates. The bedding (dip/strike) for each locality are COC (35/295), BL (32/265), BP (71/287) and BM (30/325).

component. For example, for Considerable creek basalts, these are ($D = 335.8°$, $I = -11.3°$, $\alpha_{95} = 12.2°$) and ($D = 330.9°$, $I = -8.5°$, $\alpha_{95} = 13.0°$), respectively (Table 1). This suggests that high- and mid-temperature components were acquired before and after tilting respectively, whose time interval is short compared to the plate motions or polarity reversals.

The directional results described above are in general agreement with those of the previous studies. Schmidt and Embelton (1985) sampled Mount Jope volcanics from a locality near our Beasley river locality. These rocks are of lower stratigraphy as compared to the rocks used in the present study (Thorne et al., 1995). Using a component up to 500 °C, they obtained a paleomagnetic direction of $D = 304.0°$, $I = -18.7°$ ($\alpha_{95} = 5.3°$), which is close to our in situ mid-temperature component. From fold test, they showed that this remanence was acquired during folding at early Proterozoic. A similar direction was also obtained by Schimdt and Clark (1994) using BIFs from Wittenoom and Paraburdoo BIFs, and iron ores from Parburdoo and Mount Tom Price. However, the distinction between the mid- and high-temperature components used in the present study was not made in the previous studies. The direction of the bedding corrected very high-temperature component; $D = 152.5°$, $I = 38.6°$ ($\alpha_{95} = 12.9°$), in the present study has a similar declination but a shallower inclination as compared to the bedding corrected prefolding direction determined by Schmidt and Embelton (1985); $D = 163.3°$, $I = 83.0°$ ($\alpha_{95} = 10.7°$), $D = 143.5°$, $I = 65.3°$ for two localities. Since they have also used the component over the unblocking temperature of 500 °C to determine this direction, it is likely that our very high-temperature component corresponds to their prefolding component.

5. Rock magnetism

In this section, we describe the results of rock magnetic measurements of the basalts to assess the suitability of these samples for paleointensity experiments.

An example of a room temperature measurement of a hysteresis curve under a maximum applied dc field of 300 mT is shown in Fig. 4. In the original hysteresis curve, a paramagnetic linear component dominates over the ferromagnetic component, and

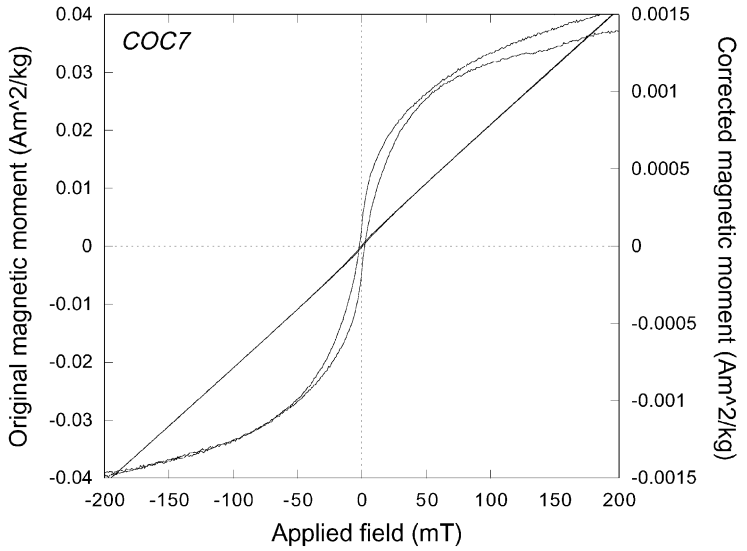

Fig. 4. An example of a hysteresis measurement for Considerable creek pillow basalt. Both the original data showing the dominance of paramagnetic linear component and the corrected data after subtracting the linear component are shown.

the loop is visible only near the origin. The slope is $0.198\,\mathrm{A\,m^2/kg\,T}$ and can be interpreted to arise from paramagnetic minerals such as silicates and pyrite (Dunlop and Özdemir, 1997). We subtract the paramagnetic component, assuming that the ferromagnetic component saturates at 200 mT, and obtain a hysteresis loop which is characterized by a constriction of loop near the origin. Tauxe et al. (1996) called this "wasp-waistedness", and showed that this type of loop forms from a mixture of superparamagnetic (SP) and single domain (SD) grains, with a SP–SD threshold of >8 nm. This indicates that these samples contain a population of very fine grains. Hysteresis parameters $J_r/J_s \simeq 0.1$, $H_c \simeq 2\,\mathrm{mT}$, are smaller than that expected for a SD magnetite, and can be explained by the wasp-waistedness. Ferromagnetic saturation magnetization is $J_s \simeq 1.5\times10^{-3}\,\mathrm{A\,m^2/kg}$, which imply a very small SD magnetite content of less than $\simeq 1.6\times10^{-5}$ in mass fraction. We have measured hysteresis properties at higher temperatures in a similar way, and determined the temperature dependence of ferromagnetic J_s (Fig. 5). This shows that the main magnetic mineral is magnetite having a Curie temperature of $\sim$590 °C.

To confirm the results of the hysteresis measurements, we have used alternative rock magnetic methods which we describe afterwards.

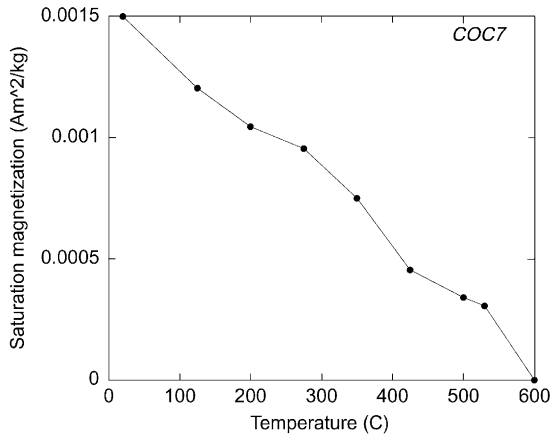

Fig. 5. Temperature dependence of saturation magnetization of ferromagnetic component determined from hysteresis curve. Specimen is the same as that used in Fig. 4.

Fig. 6 shows a result of IRM acquisition and alternating field demagnetization of ARM and SIRM performed for the same specimen. Here, IRM was acquired using an electromagnet, and an ARM was acquired under a peak alternating demagnetizing field of 100 mT and a bias dc field of 0.05 mT. IRM saturates around 300 mT and the demagnetization curves

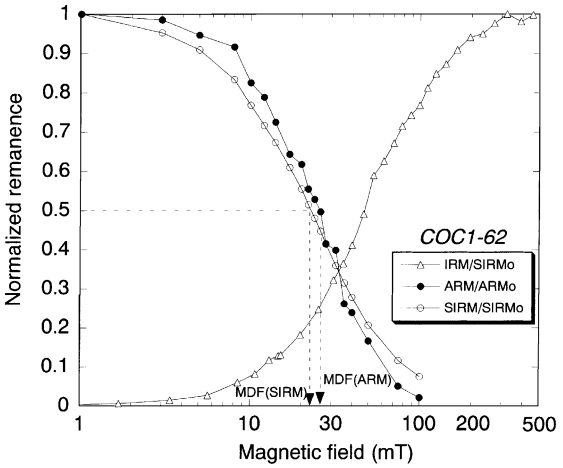

Fig. 6. IRM acquisition and alternating field demagnetization of ARM and SIRM of Considerable creek pillow basalt. The arrows indicate the mean destructive field (MDF) of ARM and SIRM.

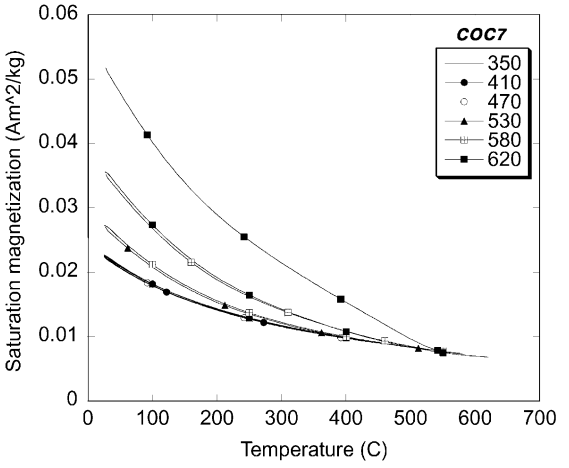

Fig. 7. Temperature dependence of saturation magnetization under a magnetic field of 100 mT for Considerable creek pillow basalt. The numbers indicate the maximum temperature (in °C) for each temperature loops.

indicate that mean destructive field (MDF) of the ARM is larger that that of SIRM. These results confirm that SD magnetite is the main remanence carrier (Lowrie and Fuller, 1971).

Susceptibility measurements show that the volume susceptibility of the basalts is $(7 \pm 2) \times 10^{-4}$ (SI). Königsberger ratio defined as

$$Q = \frac{\mathrm{NRM}}{\chi H}$$

where χ is the susceptibility, and H the present magnetic field strength of 30 μT represents the vulnerability against viscous remanence, and is of the order of 10^{-3} for these basalts. This explains the presence of significant VRM component in these rocks. A low susceptibility confirms the low ferromagnetic content in these rocks.

Fig. 7 shows the temperature dependence of saturation magnetization for Considerable creek pillow basalt. Here, a magnetic field of 100 mT was imposed, and the saturation magnetization was measured for several temperature loops up to incrementally higher temperatures. Paramagnetic component with a $1/T$ dependence is dominant. Such paramagnetism is likely to be due to the presence of silicate minerals and/or superparamagnetic magnetites. An irreversible increase of saturation magnetization is observed for 530 °C loop and higher. This can be attributed to magnetite formation from oxidation of non-magnetic silicates, as is indicated by the steepening of slope at ∼590 °C. The unblocking temperature of NRM is around 520 °C, so this result shows that magnetic mineralogy alteration is small below the blocking temperature.

We also made microscopic observation using SEM, and examples of reflection images are shown in Fig. 8. In Fig. 8A, a diagonal array of pyrite grains suggest that these rocks were subject to hydrothermal metamorphism. From probe analysis, we were able to identify minerals having composition of albite, pyrite, pumpellyite, calcite for Considerable creek pillow basalts, and quartz, titanite for Beasley river basalts. These minerals are typical of prehenite–pumpelyite to greenschist facies metamorphism, and a similar mineral assemblage is reported from deep sea drilled hydrothermally altered oceanic crust (Alt et al., 1986). We could not identify magnetite from probe analysis, indicating that they are of submicron size beyond resolution by SEM.

To summarize, rock magnetic measurements reveal that these basalts contain fine-grained, rare magnetite of SP–SD range, which alter little from heating up to their unblocking temperatures. This suggests that these rocks are good candidates for paleointensity determination.

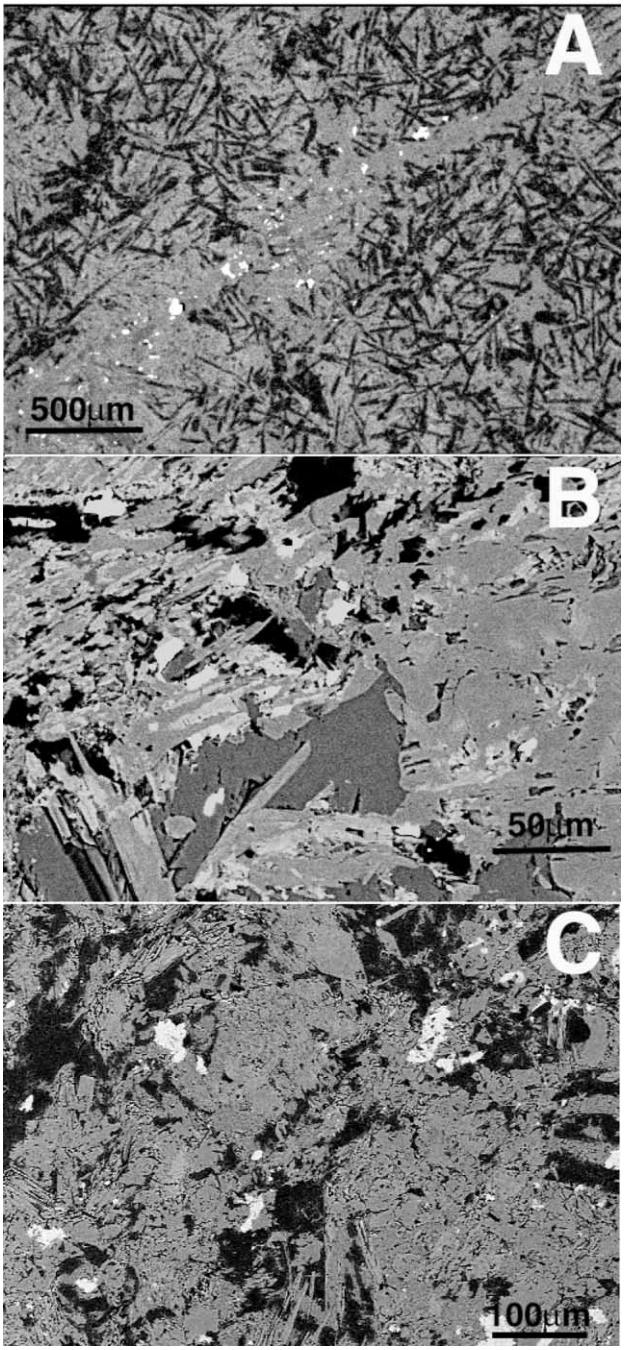

Fig. 8. An SEM reflection image of (A and B) Considerable creek and (C) Beasley river basalts: (A) a diagonal array of white grains are pyrite and dark acicular crystals are albite; (B) gray euhedral crystals are calcite; (C) white grains are titanite and the dark area are quartz.

6. Origin of remanent magnetization

It is known that Fe–Ti oxides of unmetamorphosed basalts usually have 20–50% of magnetite content in the ulvöspinel-magnetite (Fe_2TiO_4–Fe_3O_4) solid solution series (Haggerty, 1976), unlike those used in the present study. On the other hand, dredged samples from the present day oceanic ridges subject to hydrothermal activity (Smith and Banerjee, 1986; Wooldridge et al., 1990), and samples from obducted ophiolite complexes (Banerjee, 1980), show a similar rock magnetic properties as those used in the present study. These evidence suggest that fine grained Ti-free magnetites are not primary, but have been derived through greenschist metamorphism, at a condition between 300 °C at 120 MPa and 470 °C at 250 MPa (Thorne and Tyler, 1994). Through metamorphism, original titanomagnetites would have been replaced by titanite while secondary magnetite have formed from pyroxenes and olivines (Alt et al., 1986).

Based upon paleomagnetic and rock magnetic measurements, we propose the following history of the remanence magnetization acquisition for the basalts used in this study. First at ∼2.7 Ga, there is the destruction of primary magnetic minerals from greenschist facies ocean floor hydrothermal metamorphism. At the same time, there is the formation of secondary magnetite from non-magnetic minerals, resulting in a thermochemical remanence which is present as the very high-temperature component. Next, there is the acquisition of pre-tilting thermoviscous remanence (TVRM) from burial metamorphism until ∼2.1 Ga, which corresponds to the high-temperature component. Then there is the acquisition of post-tilting thermal remanence (or TVRM) from cooling during uplift at ∼2.0 Ga, which corresponds to the mid-temperature component. Finally, there is the VRM acquisition during the present magnetic polarity, resulting in a low-temperature component. We note that the mid-temperature component with a similar temperature range and direction is present in the BIFs, which we can also interpret as a remanence acquired during uplift. We discuss these sequence in more detail afterwards.

Ocean-floor hydrothermal metamorphism is likely to have been common throughout the Pilbara and Hamersley region. This is supported by the fact that

the pillow basalts from Pilbara craton where it seems to be less subjected to burial metamorphism (Smith et al., 1982), also have a similar metamorphic grade (e.g. Ohta et al., 1996). It is possible that the iron content leached from these basalts have become the source of the BIFs (e.g. Jacobsen and Pimentel-Klose, 1988; Klein and Beukes, 1992). TCRM acquired at ocean floor would have been mostly overprinted by subsequent burial, but the very high-temperature component seen in samples from site BP as well as those reported in Schmidt and Embelton (1985), is likely to be the remanence that have survived this. On the other hand, BIFs were deposited away from the mid-oceanic ridge and may not have experienced the ocean-floor hydrothermal metamorphism.

The uplift which followed the burial metamorphism, and lasted to around ∼2.0 Ga, has been interpreted to be a result of Pilbara and Yilgarn cratons gradually becoming closer (Tyler and Thorne, 1990). The time span of burial metamorphism can be estimated from the minimum laboratory unblocking temperature of the high-temperature component, which is 470 °C. Using the single domain blocking/unblocking time–temperature contours of Pullaih et al. (1975), we find that this unblocking temperature results from heating at 380 to 390 °C, a typical temperature of greenschist metamorphism, for 1–10 My.

Smith et al. (1982) showed that there is a metamorphic zoning in the Hamersley basin, with increasing degree of metamorphism to the south. He interpreted this to be the result of deeper burial depth to the south. If we follow this interpretation, then it implies that the degree of thermal overprint during burial and uplift should also have been greater in the south. In the present study, site COC is located south of sites BP, BL and the sampling sites of Schmidt and Embelton (1985). We find that none of the six hand samples from site COC and four samples from site BL show the presence of very high-temperature component, whereas three out of five hand samples from site BP, and 5 out of 15 sites of Schmidt and Embelton (1985) show the presence of this component. This is consistent with the model of Smith et al. (1982) and is an additional evidence for the origin of high- and mid-temperature components as the thermal overprint during burial and uplift, respectively.

It is possible that during burial and uplift, CRM was acquired together with TVRM and TRM, but we estimate its contribution to NRM is small for the following reasons. First, a CRM with unblocking temperature up to ∼470 °C would be mostly overprinted by TRM or TVRM. Second, if a substantial CRM acquisition occurred during uplift, then it would contaminate the whole blocking temperature spectrum, and we would not to be able to distinguish the mid-, high- and very high-temperature components on orthogonal plots, which is inconsistent with the results.

7. Paleointensity determinations

7.1. Thellier method

Following the above argument, we conclude that the mid-temperature component is the TRM, and use this component to determine paleointensity.

For all samples used to determine paleomagnetic direction, we used Coe's (1967) modified Thellier method (Thellier and Thellier, 1959) to determine the paleointensities. Susceptibility measurements at room temperature were done after each heating step. Several PTRM checks were done to monitor chemical alterations. Experiments were done under different applied laboratory fields of 10, 15, 20, 30, 40, 50, 60, 100 and 200 μT to check the proportionality.

We determined the paleointensity using the following method. First, using the orthogonal plot during the thermal demagnetization in Thellier method, we identified the mid-temperature component up to the unblocking temperature of ∼400 °C. We then performed a least squares fit from the TRM and NRM data, and narrowed the range so that it minimized σ_b/b, where b is the slope and σ_b is its standard deviation. The slope and the standard deviation thus determined were used to calculate the paleointensity estimate. The criteria for data selection are as follows: (1) more than four points should be used for paleointensity determination; (2) correlation coefficient between the TRM and NRM in the range used for paleointensity determination should be larger than 0.90; (3) PTRM checks should reproduce TRM within 15% of the previously acquired TRM at the same temperature.

Most specimens were heated for 20–25 min using Natsuhara's thermal demagnetizer which we consider allows the sample to become thermally equilibrium with the furnace temperature (Natsuhara,

Table 2
Thellier results[a]

Sample	ΔT (°C)	N	r	b	σ_b/b	f	B_{lab} (μT)	B_{paleo} (μT)
COC1-21	200–410	6	0.979	0.073	0.103	0.299	100	7.33 ± 0.76
COC1-41	200–360	5	0.990	0.056	0.082	0.153	100	5.60 ± 0.46
COC1-52	210–289	4	0.988	0.860	0.113	0.051	10	8.60 ± 0.97
COC1-61	200–410	6	0.936	0.037	0.188	0.259	100	3.73 ± 0.70
COC2-3	230–360	4	0.972	0.064	0.172	0.204	100	6.42 ± 1.10
COC4-11	350–500[b]	5	0.990	0.035	0.083	0.122	200	7.00 ± 0.58
COC4-22	330–530[b]	5	0.989	0.171	0.087	0.312	60	10.25 ± 0.89
COC4-31	200–435	8	0.973	0.251	0.098	0.357	40	10.03 ± 0.98
COC4-34	350–560[b]	6	0.990	0.073	0.072	0.192	100	7.32 ± 0.53
COC4-42	370–600[b]	6	0.960	0.135	0.145	0.507	60	8.10 ± 1.18
COC5-62	210–314	5	0.955	0.594	0.180	0.087	10	5.94 ± 1.07
COC7-51	270–540[b]	7	0.976	0.144	0.100	0.424	50	7.20 ± 0.72
BL1-52	180–277	4	0.992	1.103	0.088	0.156	15	16.54 ± 1.45
BL1-53	180–303	6	0.996	0.906	0.048	0.174	15	13.60 ± 0.65
BL1-62	200–315	5	0.983	0.241	0.109	0.145	40	9.63 ± 1.05
BL4-11	290–405	5	1.000	0.801	0.008	0.301	20	16.01 ± 0.13
BL4-71	248–380	5	0.969	0.511	0.180	0.265	30	15.34 ± 1.75
BL4-83	215–415	7	0.990	0.500	0.064	0.478	30	14.99 ± 0.96
BL4-112	215–380	6	0.988	0.405	0.078	0.246	30	12.16 ± 0.95
BP3-13	180–303	7	0.962	0.525	0.127	0.269	15	7.87 ± 1.00
BP3-32	230–315	4	0.987	0.446	0.113	0.233	20	8.91 ± 1.01
BP3-33	200–315	5	0.959	0.155	0.170	0.285	40	6.19 ± 1.05

[a] Site mean at COC (five hand samples, $N_{selected}/N_{total} = 12/29$) 6.88 ± 1.03 μT (VDM $= (1.75 \pm 0.26) \times 10^{22}$ A m^2). Site mean at BL (two hand samples, $N_{selected}/N_{total} = 7/21$) 13.94 ± 0.97 μT (VDM $= (3.59 \pm 0.25) \times 10^{22}$ A m^2). Site mean at BP (one hand sample, $N_{selected}/N_{total} = 3/13$) 7.66 ± 1.37 μT (VDM $= (1.82 \pm 0.33) \times 10^{22}$ A m^2). ΔT: temperature range; N: number of points; r: correlation coefficient between TRM and NRM; b: slope; σ_b: standard deviation of slope; f: fraction of NRM; B_{lab}: laboratory applied field; B_{paleo}: calculated paleointensity; $N_{selected}$: number of specimens selected for paleointensity determination; N_{total}: total number of specimens used for Thellier experiments.

[b] Calibrated temperature range (see text).

personal communication). Five specimens indicated by a dagger in Table 2 were heated for 10 min using Schostetd's demagnetizer, and comparing the results with those of 20–25 min heating showed that the specimen temperature was lower than the furnace temperature. For these specimens, the temperature range used was calibrated using the orthogonal plot.

7.2. Shaw method

For some samples, alternating field demagnetization was capable of separating the same multicomponents revealed by the thermal demagnetization. For these samples, Shaw method (Shaw, 1974) was done. After alternating field demagnetization, TRM was applied by heating the sample up to 590 °C. ARM check was done before and after heating, to monitor the effect of alterations. ARMs were acquired under a peak alternating field of 100 or 110, and 0.05 mT dc bias field. We identified the TRM component from the orthogonal plot, and calculated the paleointensity from the slope of NRM–TRM plot using the least squares method. Within the range used, we compared the ARM before and after heating, and rejected specimens whose correlation coefficient was <0.99.

7.3. Results

Examples of the results Thellier method are shown in Fig. 9, some with the results of susceptibility measurements and thermal demagnetization during the experiment. Summary of the results for each localities are given in Table 2. The change of susceptibility in the range used for paleointensity determination is $\simeq 7 \pm 4\%$.

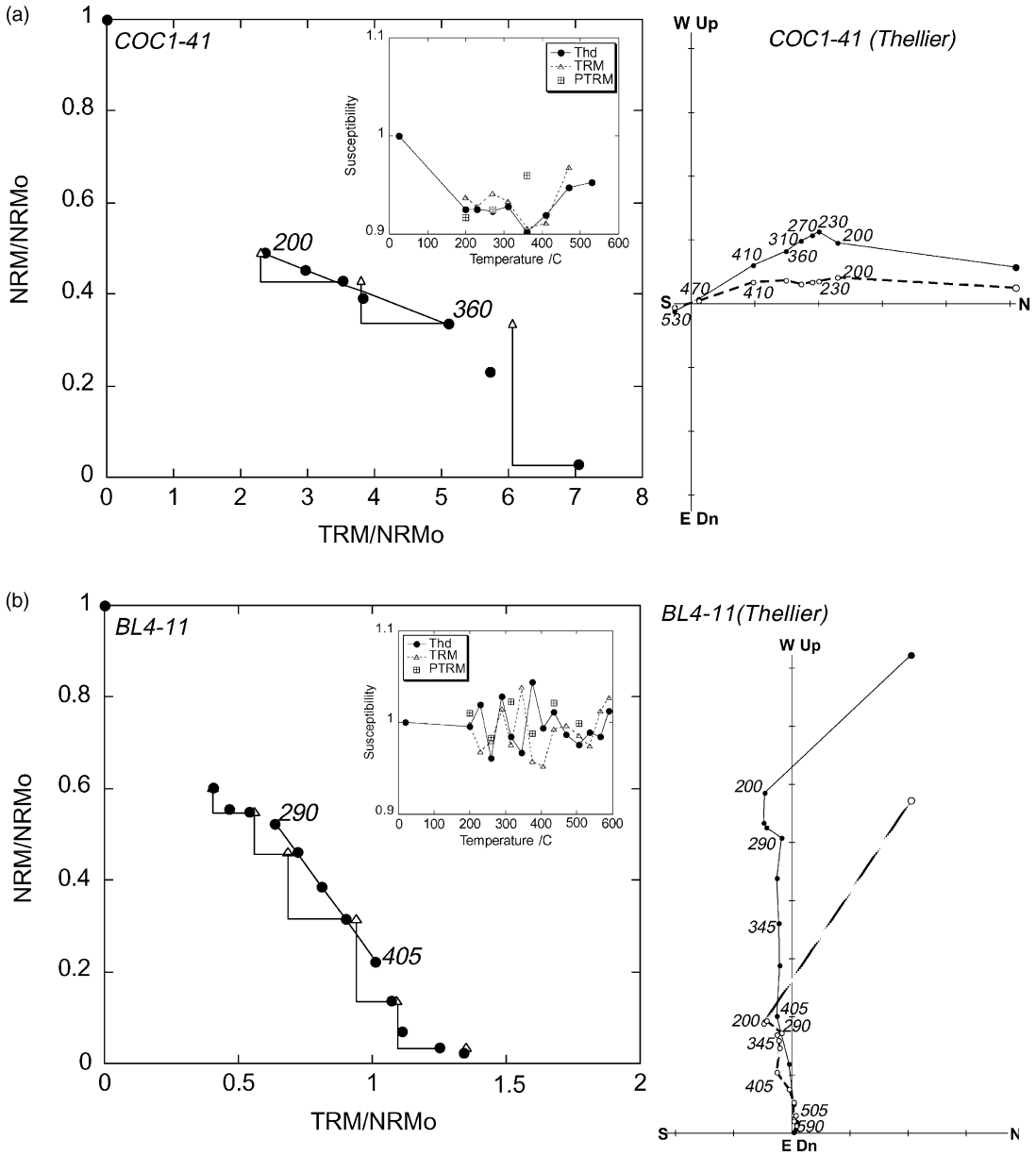

Fig. 9. Results of the Thelliers method for Considerable creek pillow basalts (a, d and e), Beasley river lava flow (b, f and g) and Beasley river pillow basalt (c). The remaining NRM and the acquired TRMs are normalized by the original NRM. The numbers indicate the temperature (in °C) and the line indicates the linear fit used for paleointensity determinations. Triangles are the results of the PTRM checks. The corresponding room temperature susceptibility measurements after each heating step, and orthogonal plots of the NRM during the experiment are shown for typical specimens from each site.

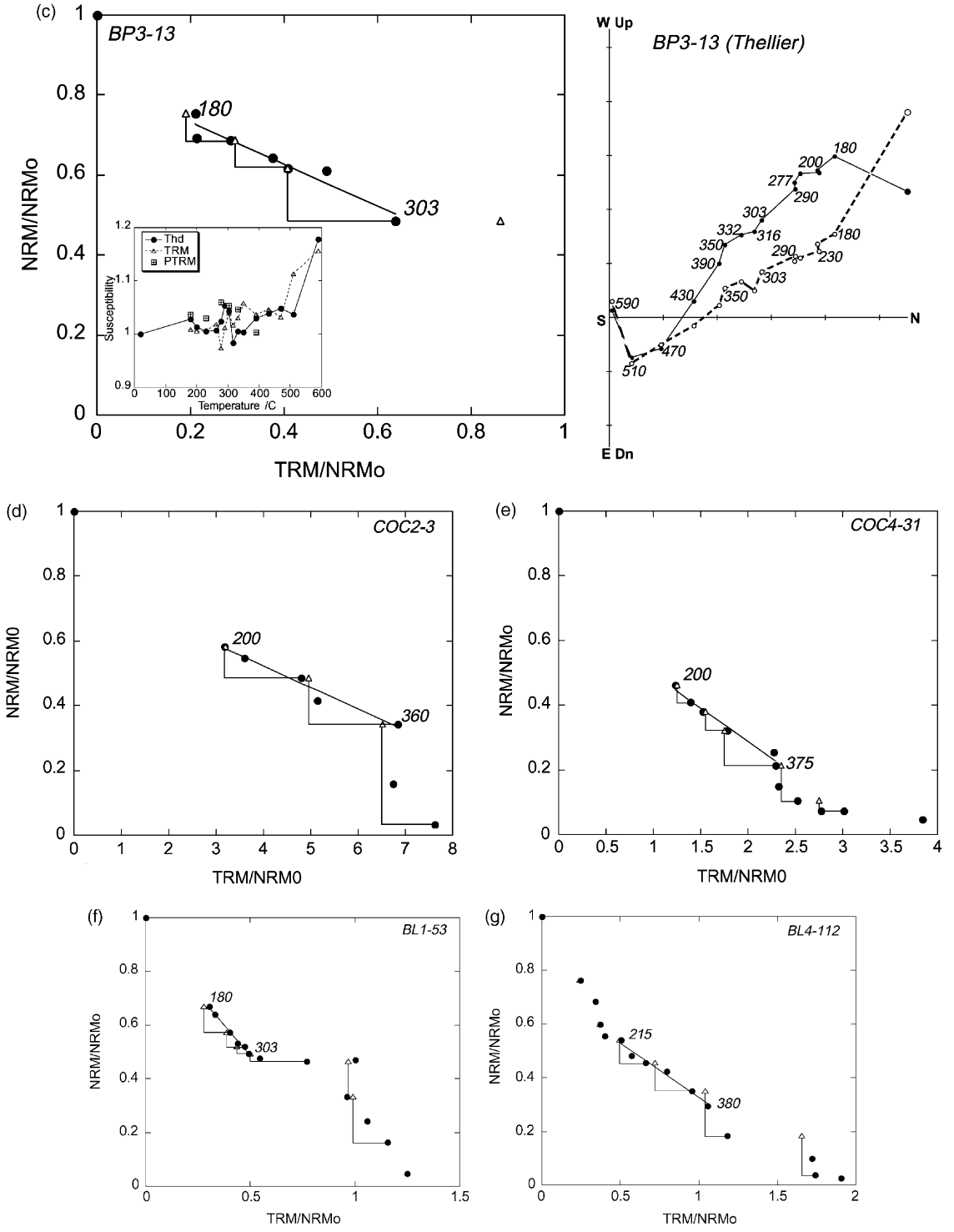

Fig. 9. (*Continued*).

From TRM–NRM plot, we find that three ranges can be identified. The most well-defined linear portion corresponds to the mid-temperature component which is used to calculate paleointensity. On the other hand, TRM–NRM plot has a steeper slope and a poorer linearity for low-temperature (VRM) and high-temperature (TVRM) components. For samples with NRM of the order of 10^{-4} A/m, accurate measurement becomes difficult as the demagnetization step proceeds, and this also contributes to the deviation from linearity. If we assume that the geomagnetic field intensity was the same during burial and uplift, a steeper slope of a high-temperature component is consistent with its TVRM origin because TVRM is estimated to be larger than TRM (Halgedahl et al., 1980). PTRM checks typically starts to fail over 400 °C, which indicates the build up of laboratory acquired CRM from non-magnetic minerals. This also suggests that these samples have not been reheated above these temperatures after burial metamorphism. If there is no break down of proportionality between the applied field and the acquired thermoremanence, the paleointensity values obtained under different laboratory fields should be the same. As can be seen from the Table 2, comparing subsamples from the same hand sample (e.g. COC1-21 and COC1-52, BP3-13 and BP3-33), this is fairly well satisfied. The linearity of the mid-temperature component and the proportionality of determined paleointensity are diagnostic of TRM. The change of susceptibility in the range used for paleointensity determination is $\simeq 7 \pm 4\%$. Specimens COC1-41 and BL4-11 do not show a clear trend of susceptibility changes during the experiment, whereas BP3-13 shows a trend of increasing susceptibility above 500 °C, which indicates a formation of magnetite from non-magnetic minerals.

The results of Shaw method are shown in Fig. 10 and Table 3. Paleointensity determined using the Shaw method is similar to that obtained from Thellier method. Fig. 11 compares the demagnetization of NRM, TRM and ARM, from which we find that there is a close similarity of the demagnetization curve above the peak demagnetization field 20 mT, where VRM component is erased. This suggests that NRM is a likely to be TRM above this demagnetization step, and also indicates that ARM can be a good analogue of TRM in these samples (Levi and Merrill, 1976).

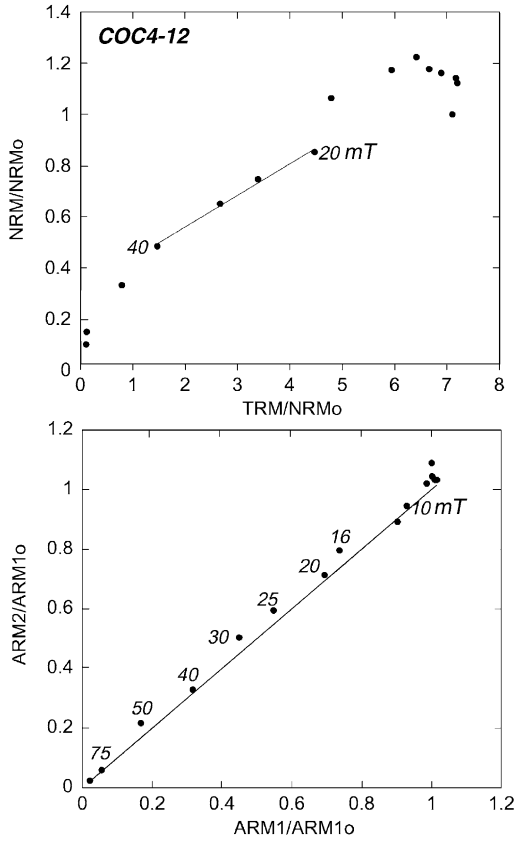

Fig. 10. Result of Shaw method for Considerable creek pillow basalt. Top: TRM–NRM plot with the linear fit used to determine the paleointensity. Numbers indicate the peak demagnetization field (in mT). Bottom: ARM checks before (ARM1) and after (ARM2) heating. The line indicates a slope of 1.

Paleointensity values obtained are all weaker than the present geomagnetic field intensity. We calculate the site mean paleointensity from the mean of the separate hand samples, and then convert to virtual dipole moment (VDM) using the inclination of the in situ mid-temperature component given in Table 1. We find that the VDM ranges from 1.8×10^{22} to 3.6×10^{22} A m^2, which is less than one-half of the present geomagnetic field intensity.

8. Discussions

Our results indicate a weak geomagnetic field at ~2.0 Ga. In Fig. 12, we plot our results and the re-

Table 3
Shaw results[a]

Sample	AFD range (mT)	N	r	b	σ_b/b	f	B_{lab} (μT)	B_{paleo} (μT)
COC4-12	20–40	4	0.996	0.124	0.061	0.369	80	9.90 ± 0.60
COC4-43	30–80	6	0.999	0.065	0.022	0.526	150	9.77 ± 0.22

[a] Mean (one hand sample, $N_{selected}/N_{total} = 2/4$) 9.84 ± 0.09 μT (VDM $= (2.51 \pm 0.02) \times 10^{22}$ A m^2).

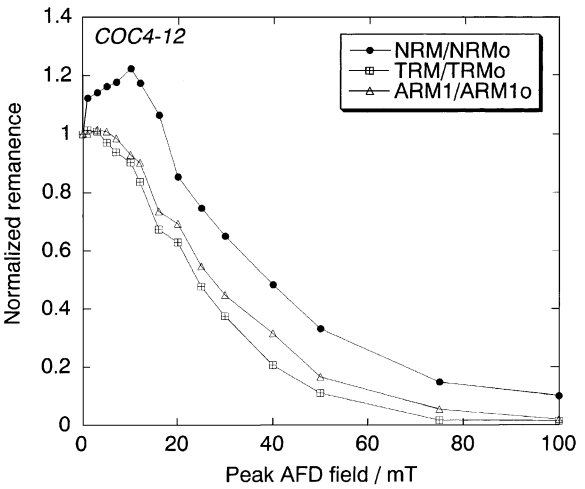

Fig. 11. Alternating field demagnetization of NRM, TRM and ARM (before heating) during the Shaw method shown in Fig. 10.

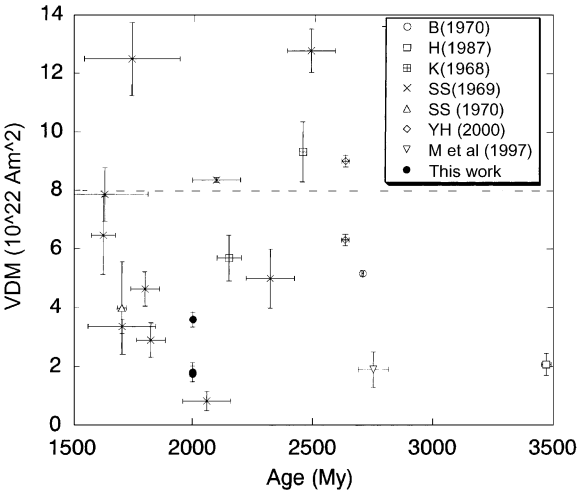

Fig. 12. VDM during Archean to early Proterozoic, determined from Thellier method. The data are compiled from an updated database of Schwartz and Symons (1970), Bergh (1970), Hale (1987), Kobayashi (1968), Schwartz and Symons (1969), Schwartz and Symons (1970), Morimoto et al. (1997), Yoshihara and Hamano (2000) and this work (in solid circles). A horizontal dashed line indicates the present VDM.

sults of Thellier experiments from Archean to early Proterozoic (3.5–1.6 Ga) from an updated version of the database of Tanaka and Kono (1994) and recent works (Morimoto et al., 1997; Yoshihara and Hamano, 2000). Despite the data scatter, we notice a low VDM intensity around 2.0 Ga. If we account for the slow cooling rate during uplift as compared to that in the laboratory, then the actual paleointensity would have been even smaller by a factor of 2 or more (Halgedahl et al., 1980). A low paleointensity around 2.0 Ga has been remarked previously (Tanaka et al., 1995), and together with our data this may indicate a globally low geomagnetic field at that time. We note that another such low VDM seem to have existed around 120–180 My (Prévot et al., 1990; Tanaka et al., 1995), which is also consistent with the recent paleointensity compilation by Selkin and Tauxe (2000). Our result is another evidence suggesting that the geodynamo with a weak VDM has occasionally existed during the Earth's history.

Our study differs from most of the previous paleointensity studies on Precambrian rocks in that we have used metamorphosed basalts with weak remanent magnetizations, rather than more strongly magnetized intrusive rocks. Our study shows that despite its very weak remanence, these rocks have an ideal grain size assemblage for paleointensity studies. In the present case, the paleomagnetic directions of these rocks recorded the tectonic changes related to the possible collision between the cratons, and was useful for constraining the timing of the remanence acquisition. These basalts are common in the Archean granite-greenstone terranes, and may be used to further unravel the nature of the ancient geomagnetic field, and the tectonic history of the region.

9. Conclusions

1. Thermal demagnetization shows that 2.7 Ga basalts (pillows and lava flows) and 2.5 Ga BIFs of Hamersley basin have two to four components of stable magnetization. The low- and mid-temperature components are present in all samples and have consistent directions.
2. Rock magnetic measurements of basalts indicate the presence of fine-grained (SP–SD), rare magnetite, which we interpret to have been derived from greenschist metamorphism. Thermomagnetic analyses show reversible behavior up to its unblocking temperature.
3. We interpret the high-temperature component up to $\sim$500 °C as a pre-tilting thermoviscous remanence acquired during burial, and the mid-temperature component up to $\sim$390 °C as a post-tilting thermal overprint during uplift which ended at $\sim$2.0 Ga.
4. Thellier paleointensity experiments with consistency checks for three sites (22 specimens) yield a weak paleointensity estimate with a VDM of $(1.8–3.6) \times 10^{22}$ A m^2 at $\sim$2.0 Ga.

Acknowledgements

We thank S. Maruyama and his colleagues for their guidance and help during the sampling trips and throughout the course of this study. We thank A. Thorne, D. Nelson and the Geological Survey of Western Australia for their support and discussions, and two anonymous referees for their helpful comments on the manuscript. Part of this study was supported by the Decoding the Earth Evolution Program, Intensified Study Area Program of Ministry of Culture and Education (No. 259, 1995–1997) and Japan Society for the Promotion of Science Research Fellowships for Young Scientists (I.S., T.H., A.Y.).

References

Alibert, C., McCulloch, M.T., 1993. Rare-earth element and neodymium isotopic compositions of the banded iron-formations and associated shales from Hamersley, Western Australia. Geochim. Cosmochim. Act. 57, 187–204.

Alt, J.C., Honnorez, J., Laverne, C., Emmermann, R., 1986. Hydrothermal alteration of a 1 km section through the upper oceanic crust, deep sea drilling project hole 504B: mineralogy, chemistry, and evolution of seawater-basalt interactions. J. Geophys. Res. 91, 10309–10335.

Arndt, N.T., Nelson, D.R., Compston, W., Trendall, A.F., Thorne, A.M., 1991. The age of the Fortescue Group, Hamersley basin, Western Australia, from ion microbe zircon U–Pb results. Aust. J. Earth Sci. 38, 181–261.

Banerjee, S.K., 1980. Magnetism of the oceanic crust: evidence from ophiolite complexes. J. Geophys. Res. 85, 3557–3566.

Bergh, H.W., 1970. Paleomagnetism of the stillwater complex, Montana. In: Runcorn, S.K. (Ed.), Paleogeophysics. Academic Press, London, pp. 143–158.

Coe, R.S., 1967, Paleo-intensities of the Earth's magnetic field determined from tertiary and quaternary rocks. J. Geophys. Res. 72, 3247–3262.

Dunlop, D.J., Özdemir, Ö., 1997. Rock Magnetism. Cambridge University Press, Cambridge, MA, 573 pp.

Embleton, B.J.J., 1978. The Paleomagnetism of 2400 My rocks from the Australian Pilbara craton and its relation to Archean-Proterozoic Tectonics. Precamb. Res. 6, 275–291.

Embleton, B.J.J., Robertson, W.A., Schmidt, P.W., 1979. A survey of magnetic properties of some rocks from North Western Australia. Investigation Report 129, Institute of Earth Resources, CSIRO, Australia.

Erel, Y., Harlavan, Y., Stein, M., Blum, J.D., 1997. U–Pb dating of Fe-rich phases using a sequential leaching method. Geochim. Cosmochim. Act. 61, 1697–1703.

Haggerty, S.E., 1976. Oxidation of opaque mineral oxides in basalts. In: Rumble III, D. (Ed.), Review of Mineralogy, Vol. 3. Mineralogical Society of America, Washington, DC, 502 pp.

Hale, C.J., 1987. The intensity of the geomagnetic field at 3.5 Ga: paleointensity results from the Komati formation, Barberton Mountain Land, South Africa. Earth Planet. Sci. Lett. 586, 354–364.

Halgedahl, S.L., Day, R., Fuller, M., 1980. The effect of cooling rate on the intensity of weak-field TRM in single-domain magnetite. J. Geophys. Res. 85, 3690–3698.

Hatakeyama, T., Sata, N., Hamano, Y., 1997. Paleomagnetism and rockmagnetism of Proterozoic banded iron formation in the Hamersley province, Western Australia. Eos Suppl. Trans. AGU 78, F171.

Hickman, A.H., 1983. Geology of the Pilbara block and its environs. Geol. Surv. West. Aust. Bull. 127, 268.

Jacobsen, S.B., Pimentel-Klose, M.R., 1988. An Nd isotopic study of the Hamersley and Michipicoten banded iron formations: the source of REE and Fe in Archean oceans. Earth Planet. Sci. Lett. 87, 29–44.

Klein, C., Beukes, N.J., 1992. Proterozoic iron-formations. In: Condie, K.C. (Ed.), Proterozoic Crustal Evolution. Elsevier, Amsterdam, pp. 383–418.

Kobayashi, K., 1968. Paleomagnetic determination of the intensity of the geomagnetic field in the Precambrian period. Phys. Earth Planet. Inter. 1, 387–395.

Levi, S., Merrill, R.T., 1976. A comparison of ARM and TRM in magnetite. Earth Planet. Sci. Lett. 32, 171–184.

Lowrie, W., Muller, M., 1971. On the alternating field demagnetization characteristics of multidomain thermoremanent magnetization in magnetite. J. Geophys. Res. 76, 6339–6349 .

McElhinny, M.W., Senanayake, W.E., 1980. Paleomagnetic evidence for the existence of the geomagnetic field 3.5 Ga ago. J. Geophys. Res. 85, 3523–3528.

Morimoto, C., Otofuji, Y., Miki, M., Tanaka, H., Itaya, T., 1997. Preliminary paleomagnetic results of an Archean dolerite dyke of west Greenland: geomagnetic field intensity at 2.8 Ga. Geophys. J. Int. 128, 585–593.

Nelson, D.R., Trendall, A.F., de Laeter, J.R., Grobler, N.J., Fletcher, I.R., 1992. A comparative study of the geochemical and isotopic systematics of late Archean flood basalts from the Pilbara and Kaapvaal cratons. Precamb. Res. 54, 231–256.

Ohta, H., Maruyama, S., Takahashi, E., Watanabe, Y., Kato, Y., 1996. Field Occurrence, Geochemistry and Peterogenesis of the Archean mid-oceanic ridge basalts (AMORBS) of the Cleaverville area, Pilbara craton, Western Australia. Lithos 37, 199–221.

Porath, H., Chamalaun, F.H., 1968. Paleomagnetism of Australian haematite orebodies. II. Western Australia. Geophys. J. R. Astron. Soc. 15, 253–264.

Prévot, M., Perrin, M., 1992. Intensity of the Earth's magnetic field since Precambrian from Thellier-type paleointensity data and inferences on the thermal history of the core. Geophys. J. Int. 108, 613–620.

Prévot, M., Deder, M.M., McWilliams, M., Thompson, J., 1990. Intensity of the Earth's magnetic field: evidence for a Mesozoic dipole low. Earth Planet. Sci. Lett. 97, 129–139.

Pullaiah, G., Irving, E., Buchan, K.L., Dunlop, D.J., 1975. Magnetization changes caused by burial and uplift. Earth Planet. Sci. Lett. 28, 133–143.

Schmidt, P.W., Clark, D.A., 1994. Paleomagnetism and magnetic anisotropy of Proterozoic banded iron formations and iron ores of the Hamersley basin, Western Australia. Precamb. Res. 69, 133–155.

Schmidt, P.W., Embelton, B.J.J., 1985. Prefolding and overprint magnetic signatures in Precambrian (∼2.9–2.7 Ga) Igneous rocks from the Pilbara craton and Hamersley basin, NW Australia. J. Geophys. Res. 90, 2967–2984.

Schwartz, E.J., Symons, D.T.A., 1969. Geomagnetic intensity between 100 and 2500 million years ago. Phys. Earth Planet. Inter. 2, 11–18.

Schwartz, E.J., Symons, D.T.A., 1970. Paleomagnetic field intensity during cooling of the Sudbury Irruptive 1700 million years ago. J. Geophys. Res. 75. 6631-6640.

Selkin, P.A., Tauxe, L., 2000. Long-term variations in palaeointensity. Phil. Trans. R. Soc. London. 358, 1065–1088.

Shaw, J., 1974. A new method of determining the magnitude of the paleomagnetic field application to five historic lavas and five archeological samples. Geophys. J. R. Astron. Soc. 39, 133–141.

Smith, G.M., Banerjee, S.K., 1986. Magnetic structure of the upper kilometer of the marine crust at deep sea drilling project hole 504B, Eastern Pacific Ocean. J. Geophys. Res. 91, 10337–10354.

Smith, R.E., Perdrix, J.L., Parks, T.C., 1982. Burial metamorphism in the Hamersley basin, Western Australia. J. Petrol. 23, 75–102.

Tanaka, H., Kono, M., 1994. Paleointensity database provides new resource. Eos. Trans. Am. Geophys. Univ. 75, 498 .

Tanaka, H., Kono, M., Uchimura, H., 1995. Some global features of paleointensity in geological time. Geophys. J. Int. 120, 97–102.

Tauxe, L., Mullender, T.A.T., Pick, T., 1996. Potbellies, wasp-waists, and superparamagnetism in magnetic hysteresis. J. Geophys. Res. 101, 571–583.

Thellier, E., Thellier, O., 1959. Sur l'intensite du champ terrestre dans le passe historique et geologique. Ann. Geophys. 15, 285–376.

Thorne, A.M., Tyler, I.M., 1994. Geology of the Paraburdoo 1:100,000 sheet. Geol. Surv. West. Aust., Perth.

Thorne, A.M., Tyler, I.M., Blight, D.F., 1995. Rocklea, W.A., West. Aust. Geol. Surv., 1:100,000 Geological Series.

Trendall, A.F., Compston, W., Williams, I.S., Armstrong, R.A., Arndt, N.T., McNaughton, N.J., Nelson, D.R., Barley, M.E., Beukes, N.J., de Laeter, J.R., Retief, E.A., Thorne, A.M., 1990. Precise U–Pb geochrnological comparison of the volcano-sedimentary sequences of the Kaapvaal and Pilbara cratons between about 3.1 and 2.4 Ga. In: Proceedings of the Third International Archaean Symposium, Perth. Extended Abstracts, pp. 81–83.

Tyler, I.M., Thorne, A.M., 1990. The northern margin of the Capricorn Orogen, Western Australia—an example of an early Proterozoic collision zone. J. Struct. Geol. 12, 685–701.

Wooldridge, A.L., Haggerty, S.E., Rona, P.A., Harrison, C.G.A., 1990. Magnetic properties and opaque mineralogy of rocks from selected seafloor hydrothermal sites at oceanic ridges. J. Geophys. Res. 95, 12351–12374.

Yoshihara, A., Hamano, Y., 2000. Intensity of the Earth's magnetic field in late Archean obtained from diabase dikes of the Slave Province, Canada. Phys. Earth Planet. Inter. 117, 295–307.